

## Article

# Removal of Phenolic Compounds from Olive Mill Wastewater by a Polydimethylsiloxane/oxMWCNTs Porous Nanocomposite

Antonio Turco <sup>1,2,\*</sup> and Cosimino Malitesta <sup>1,\*</sup> 

<sup>1</sup> Department of Biological and Environmental Sciences and Technologies (Di.S.Te.B.A.), University of Salento, Via Monteroni, 73100 Lecce, Italy

<sup>2</sup> CNR-NANOTEC Institute of Nanotechnology, Via Monteroni, 73100 Lecce, Italy

\* Correspondence: antonio.turco@nanotec.cnr.it (A.T.); cosimino.malitesta@unisalento.it (C.M.)

Received: 13 November 2020; Accepted: 7 December 2020; Published: 10 December 2020



**Abstract:** User-friendly and energy-efficient methods able to work in noncontinuous mode for *in situ* purification of olive mill wastewater (OMW) are necessary. Herein we determined the potential of oxidized multiwalled carbon nanotubes entrapped in a microporous polymeric matrix of polydimethylsiloxane in the removal and recovery of phenolic compounds (PCs) from OMW. The fabrication of the nanocomposite materials was straightforward and evidenced good adsorption capacity. The adsorption process is influenced by the pH of the OMW. Thermodynamic parameters evidenced the good affinity of the entrapped nanomaterial towards phenols. Furthermore, the kinetics and adsorption isotherms are studied in detail. The presence of oil inside the OMW can speed up the uptake process in batch adsorption experiments with respect to standard aqueous solutions, suggesting a possible use of the nanocomposite for fast processing of OMW directly in the tank where they are stored. Moreover, the prepared nanocomposite is safe and can be easily handled and disposed of, thus avoiding the presence of specialized personnel. After the adsorption process the surface of the nanomaterial can be easily regenerated by mild treatments with diluted acetic acid, thus permitting both the recyclability of the nanomaterial and the recovery of phenolic compounds for a possible use as additives in food and nutraceutical industries and the recovery of OMW for fertirrigation.

**Keywords:** olive mill wastewater; carbon nanotubes; polydimethylsiloxane; waste treatment; phenolic compounds; resources recovery

## 1. Introduction

Olive mill wastewater (OMW) is an acid waste derived from olive pressing, which has a production range from 10 to 30 million of m<sup>3</sup> per year [1]. OMW is composed of water, oil, and solids and exhibits ecotoxic and phytotoxic properties due to its high content of phenols [2]. For that reason, OMW has been considered as a matter of treatment and minimization [3]. However, it could represent a cheap source of components that can be recovered and used as natural food additives [4,5]. For instance, at low concentrations, phenols of olive have antioxidant properties with potential benefits for the health [6–8]. Moreover, OMW purified from phenols can be a valuable source for fertirrigation [9].

Different methods have been developed to purify OMW from phenols such as electrochemical oxidation [10], physical methods [11], solvent extraction [12], chemical treatments [13–15], filtration [16], and bioremediation [17,18]. However, these techniques could require high energy, the use of chemicals, and could generate secondary pollutants during the remediation process [19]. Moreover, phenolic compounds (PCs) could be degraded during the treatment thus not permitting their recovery. For all these reasons, there is an urgent need to develop alternative methods for the removal and

recovery of PCs from OMW. In this view, adsorption techniques can be an attractive alternative [20–25]. Different adsorbents have been developed, such as granular activated carbon [20], zeolites [26], agricultural wastes [3], and amberlite [27]. One of the major issues is that these materials are in powder form requiring large centrifuges or filtration systems for their management during the treatment. Another approach could be to pack the powder in a column for a continuous flow separation in a plant [21]. However, the seasonal production of OMW and the necessity to collect and transport OMW from the large number of olive mills to the plant can make such systems expensive [19]. Recently we have developed a nanocomposite material in which oxidized carbon nanotubes (oxCNTs) were physically entrapped on the surface of porous polydimethylsiloxane (PDMS) for the removal of phenolic compounds from aqueous solutions with good adsorption capacity. The nanocomposite can be easily handled and disposed of, making easier its recovery after the adsorption process [28]. Although the use of the material to remove phenolic compounds for OMW treatment was suggested a complete characterization of the adsorption process was not performed. In the present work we tested the ability of PDMS/oxidized multiwalled carbon nanotubes (oxMWCNTs)—spongeous materials to remove phenolic compounds from complex matrices such as OMW. The adsorption mechanisms, thermodynamic parameters, and kinetics were studied with different theoretical models. A good and fast adsorption capacity was observed. The system was demonstrated to be effective for the purification of complex OMW matrices in batch samples, suggesting their possible use for *in situ* purification of OMW, being able to work directly in the tank where the waste is stored. It has been demonstrated that the different phenols present in OMW can affect the adsorption process with respect to our previous observations. Moreover, the presence of oil in OMW can speed up the uptake process, probably due to the swelling of the pores inside the adsorbent phase. The reusability of the nanocomposite and the possibility of recovering adsorbed phenols was also demonstrated.

## 2. Materials and Methods

### 2.1. Materials

Multiwalled carbon nanotubes with a diameter of  $25.4 \pm 4$  nm were provided by Nanostructured & Amorphous Materials, Inc., Los Alamos, NM, USA. The PDMS polymerization kit (Sylgard 184), comprising monomer and curing agent, were purchased from Dow Corning, Midland, MI, USA. All the other reagents were analytical grade and purchased from VWR International srl, Milano, Italy, and used as received.

### 2.2. OMW Origin and Composition

OMW was obtained from a three-phase continuous extraction unit in Miggiano, Italy. The pH at 25 °C was equal to 4.8 and the density  $1.08 \pm 0.02$  g/L. Total suspended solids were  $2.57 \pm 0.05$  g/L, the total solids were  $25.12 \pm 0.8$  g/L, the mineral matter was  $4.02 \pm 0.07$  g/L. The phenolic amount equal to  $2.089 \pm 0.01$  g/L was calculated by Folin–Ciocalteu assay [29].

### 2.3. Preparation of the Spongeous Adsorbent

A sponge of polydimethylsiloxane (PDMS), in which oxidized multiwalled carbon nanotubes (oxMWCNTs) were stably entrapped and homogeneously dispersed on pores' surfaces, was prepared following our well-developed procedure [28]. Briefly, microparticles of glucose crystals with an average dimension of  $290 \pm 170$  µm were mixed with a shaker overnight with pristine MWCNTs at 3% *w/w*. The obtained mixture was packed in a centrifuge tube and an appropriate amount of PDMS prepolymer mixed with curing agent in the ratio of 10:1 and diluted with 40% in *wt.*% of hexane was added on the top. The composites were centrifuged at 8000 rpm for 20 min to allow the packing of the mixture and the permeation of the prepolymerization solutions between the sugar particles. The composite was then cured at 60 °C overnight to accomplish the polymerization. Finally, glucose was removed by

firstly soaking the nanocomposite in boiling water under continuous stirring and then by sonication in warm water and ethanol.

MWCNTs entrapped in the nanocomposites were then oxidized. The sponges were placed in water under reduced pressure to allow the permeation of the solution in the pores of the hydrophobic nanocomposite, then nitric acid was added until a concentration of 3 M was reached and left for two hours under continuous stirring. At the end of the process the as-obtained nanocomposites were washed repetitively with water until the pH of the washing solution remained stable. The nanocomposites were dried under vacuum and dipped in H<sub>2</sub>O<sub>2</sub> 30% *w/w* solution under stirring for 2 h. Finally, the obtained materials (PDMS/oxMWCNTs) were repetitively washed in water and dried at 100 °C overnight.

#### 2.4. Determination of PCs in OMW

The PCs in the OMW were quantified by Folin–Ciocalteu assay [29]. 240 µL of water, 50 µL of OMW, and 250 µL of Folin–Ciocalteu reagent were added in a flask. After 120 s, 2.7 mL of sodium carbonate (20% *w/v*) was added. The mixture was left at 25 °C for 2 h and then centrifuged at 8000 rpm for 5 min. The absorbance of the supernatant was read at 765 nm with a Cary UV 50 spectrophotometer. Gallic acid was used as a standard for the calibration of the method.

#### 2.5. Adsorption Experiments

A proper amount of the PDMS/oxMWCNTs nanocomposite (6 g/100 mL) was immersed in 5 mL of OMW diluted with water (pH = 4.8) with a known concentration of phenols (1.251 g/L) and shaken at 25 °C. Studies at different pH were performed, adjusting the pH with 0.1 M HCl or 0.1 M NaOH. The adsorption rates of phenols were monitored at different times (namely 0, 0.5, 1, 1.5, 2, 2.5, 3, 4, 22, and 24 h) collecting small aliquots from the solution for further spectrophotometric analysis. Removal efficiency (Q%) and equilibrium adsorption capacity ( $q_e$ ) of the sponges were calculated by Equations (1) and (2) respectively:

$$\text{removal efficiency (\%)} = \left[ \frac{(C_0 - C_t)}{C_0} \right] \times 100 \quad (1)$$

$$\text{adsorption capacity, } q_e \left( \frac{\text{mg}}{\text{g}} \right) = \left[ \frac{(C_0 - C_e)}{W} \right] \times V \quad (2)$$

where  $C_0$  and  $C_t$  are respectively the concentration of PCs at the beginning of the experiment and at a given time (hours) in ppm (mg/L),  $C_e$  is the PCs concentrations (ppm) at the equilibrium (24 h),  $W$  is the weight of the sponge in grams, and  $V$  is the volume of the solution in liters.

#### 2.6. Desorption Experiments

The adsorbent was separated from the OMW solution and washed with water. Desorption experiments were conducted by dipping the PDMS/oxMWCNTs sponge in 10% acetic acid, which was vortexed for 2 h.

### 3. Results and Discussion

#### 3.1. Adsorption of OMW PCs on PDMS/oxMWCNTs Sponges

Our developed fabrication route described in experimental methods can easily allow the synthesis of black porous PDMS/oxMWCNTs sponges (Figure 1a) in which the pores dimensions are comparable to that of the used hard template. The carbon nanotubes are well-dispersed in the polymeric matrices thanks to the mechanical destroying of  $\pi$ - $\pi$  stacking during the fabrication steps. Moreover, the oxidation of the nanomaterials in the sponges occurred after the synthesis of the 3D nanocomposites thus reducing the need of complex apparatus thanks to the easy handle of the material [28,30]. Although it is known that treatment with strong acid can degrade PDMS matrices [31], it is interesting to note as the oxidation procedure did not significantly affect the mechanical stability of the material.

This is probably due to the low concentration of nitric acid and short time of incubation used for the synthetic procedure. The prepared sponges were dipped in an OMW solution at pH 4.8 and the adsorption of PCs was monitored at different times. As reported in Figure 1c, at the beginning of the process we observed a fast phenols adsorption. After 4 h the adsorption process become slower due to the decrease in the number of easily accessible sites on oxMWCNTs [3,28,32]. Finally, for times higher than 20 h an equilibrium between the adsorbent and adsorbate is achieved. Moreover, we observed that the adsorption of PCs did not occur in 24 h on porous PDMS prepared following the procedure in Section 2.3, but in the absence of MWCNTs, and is very low on a spongy nanocomposite in which MWCNTs were not oxidized (removal efficiency approximately 2%) (data not shown).

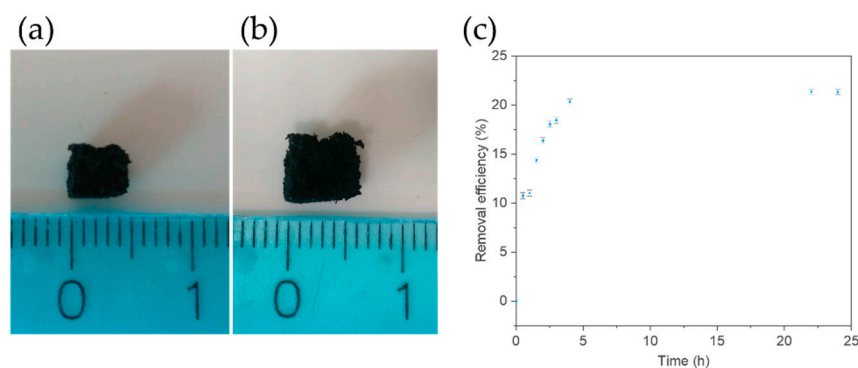


**Figure 1.** A piece of polydimethylsiloxane/oxidized multiwalled carbon nanotubes (PDMS/oxMWCNTs) sponge (a) before and (b) after dipping in an olive mill wastewater (OMW) solution. (c) Effect of contact time on adsorption of OMW phenolic compounds (PCs) on the PDMS/oxMWCNTs sponge.

Interestingly, most of the uptake process (around 95%) was completed in 4 h, evidencing a faster uptake with respect to what we observed in aqueous solutions [28].

We hypothesized that this can be due to two different reasons: on one hand it could be due to an increased affinity of phenols contained in the OMW with the adsorbent; on the other hand, it could be due to the presence of oil in the OMW, which could cause the swelling of the PDMS/oxMWCNTs sponge [30,33] thus favoring the diffusion of the mixture inside the adsorbent phase. To verify the first hypothesis the PDMS/oxMWCNTs sponge was dipped in two different solutions containing two different PCs, namely 4-nitrophenol and phenol, for which the nanomaterial has evidenced different affinities at the same concentration (i.e., 0.18 mM) [28]. We observed a significant increment in the removal efficiency at equilibrium, but not in the rate of adsorption. In fact, 84% of the process is completed in 4 h in both cases (Figure S1). Therefore, the increment in the adsorption rate was attributed to the evident swelling of the nanocomposite in OMW (Figure 1b).

### 3.2. Effect of pH and Adsorbent Amount on PCs Adsorption

pH can affect both the adsorption mechanisms and the nature of soluble species' interactions with the adsorbents [34].

We tested the pH effect on the PCs removal from OMW with our porous nanocomposite. As visible in Figure 2, the removal efficiency (%) increases from pH 2 to 4.8, then slightly decreases for pH values up to 6.5 and finally decreases dramatically at higher pH, reaching a removal efficiency (%) close to zero at pH over 10.5.

The increment in removal efficiency observed until pH of around 6.5 is mainly due to  $\pi$ - $\pi$  interactions. Although this mechanism is still not clear, it is well known that higher pH values can alter the  $\pi$  donation strength of PCs thus causing an increase of their adsorption on the oxMWCNTs' surface [28,35]. However, the removal efficiency decreased very fast at pHs over 6.5 with an apparent different behavior to that observed in adsorption of PCs on oxMWCNTs in aqueous solutions [28]. A similar behavior was also reported for some PCs adsorbed by MWCNTs [35], demonstrating that

the decreased removal efficiency of phenols for pH over their pKa could be due to the increased electrostatic repulsion between the dissociated phenols and negatively charged oxMWCNTs. Moreover, the dissociation of the PCs would increase their hydrophilicity, thus decreasing their adsorption. Consequently, the observed trend can be explained by the fact that most of the PC constituents of OMW are deprotonated at higher pH, due to their pKa lower than 5 (Figure 3) [36]. This suggests also that the adsorption of different type of phenols could be achieved at different pHs.

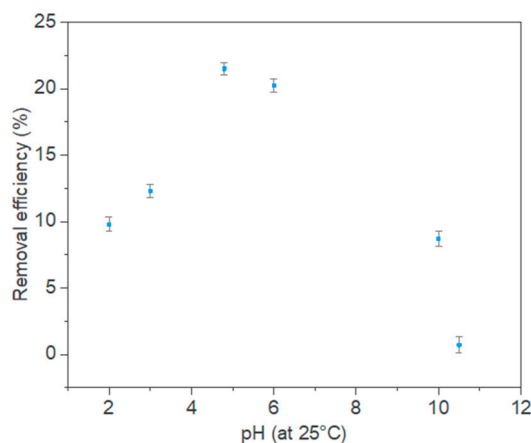


**Figure 2.** Effect of pH on adsorption of PCs by the PDMS/oxMWCNTs sponge.

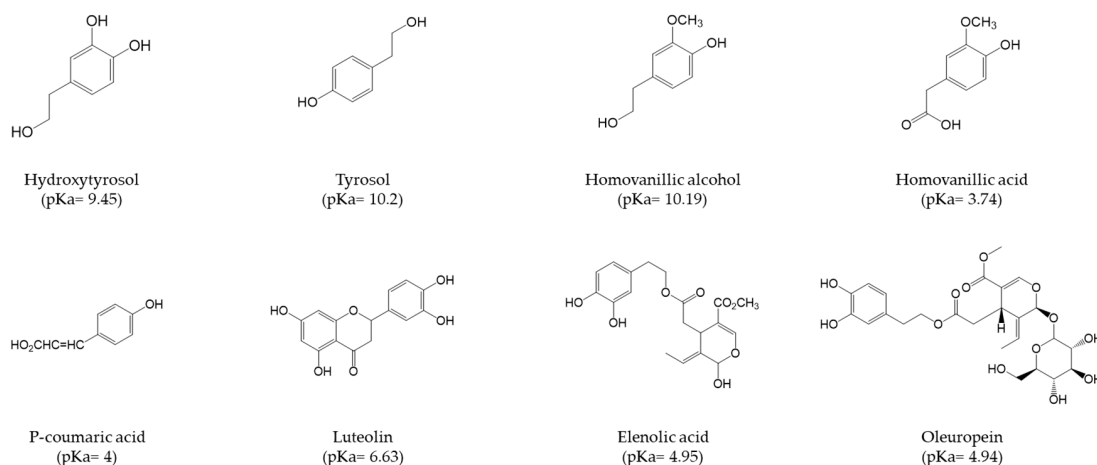


**Figure 3.** The major constituents of OMW. The common name and the pKa value are reported under each compound.

Figure 4 shows the removal efficiency (%) and adsorption capacity ( $q_e$ ) of phenols in OMW as a function of the PDMS/oxMWCNTs sponge amount in the given conditions. It is evident that an increase in sponge amount in the mixture results in an obvious increase in the phenol adsorption percent. With the increase in PDMS/oxMWCNTs amount from 4 to 10 g/100 mL, the phenol removal efficiency increased rapidly from 20.2 to 35.5%. This was intuitively due to the increase in the number of adsorption sites with the increase in the sponge amount. The results indicated that it was possible to remove phenols completely from OMW when there was a high enough PDMS/oxMWCNTs sponge amount in the mixture. On the other hand, the  $q_e$  was high at low doses and reduced at high doses, thus suggesting that some adsorption sites remain unsaturated during the adsorption process [3,37–40].

The results of this section also indicated that, in order to obtain the optimal adsorbent dosage, higher initial phenol concentrations should be tested in conjunction with appropriate adsorbent dosage depending on the concentration of phenolic compound in OMW [37,38].

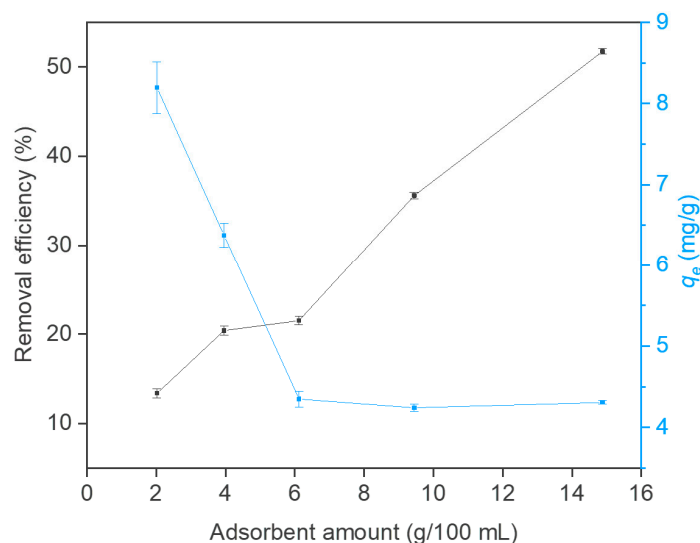


**Figure 4.** Influence of foam concentration on removal efficiency and adsorption capacity of phenolic compounds in OMW.

### 3.3. Adsorption Isotherms and Thermodynamic Parameters

Several models have been used to describe adsorption equilibrium, among which the Freundlich and the Langmuir models are the most frequently used.

The Freundlich isotherm [41] describes a reversible process in which the adsorption can occur through homogeneous and/or heterogenous interactions.

The linear form of the equation is:

$$\log q_e = \log K_F + \frac{1}{n} \log C_e \quad (3)$$

where  $K_F$  is the Freundlich constant representative of the adsorption capacity of adsorbent and  $n$  describes the strength of adsorption. An  $R^2$  of 0.80 was obtained by linear fitting (Figure S2), evidencing that the model did not describe well the experimental data, thus being in contrast with what was observed in aqueous solutions [28]. We ascribe this behavior to the complexity of OMW in which other interferences species can influence the adsorption mechanisms.

Experimental data were also fitted with the Langmuir theory [42], which is valid for monolayer adsorption onto surfaces with homogenous binding sites.

The linearized form of the isotherm is:

$$\frac{C_e}{q_e} = \frac{1}{K_L q_{max}} + \frac{C_e}{q_{max}} \quad (4)$$

where  $K_L$  (L/mg) is the Langmuir constant and is representative of the affinity of the sorbate for the sorbent and  $q_{max}$  (mg/g) is the maximum adsorption capacity.

The  $R^2$  value higher than 0.99 suggests that the model is more appropriate to describe the adsorption process. From the fitting, a  $q_{max}$  of 4.39 mg/g was found. The dimensionless equilibrium parameter ( $R_L$ ) was calculated as in Equation (5) at different concentrations of PCs.

$$R_L = \frac{1}{1 + K_L C_0} \quad (5)$$

The results summarized in the table of Figure 5 evidenced that the  $R_L$  value is always comprised between 0 and 1, confirming the high affinity of PDMS/oxMWCNTs sponge for phenols contained in OMW [3].



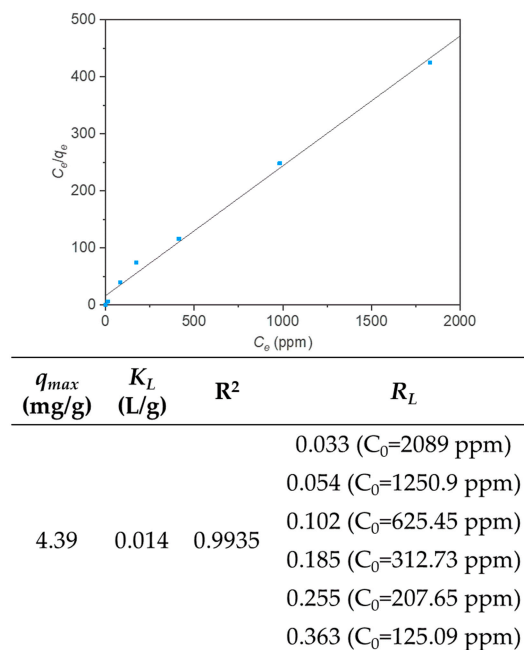


**Figure 5.** Fitting of experimental data with the linearized Langmuir isotherm model for phenols in OMW. The table reports calculated values from Equations (6) and (7).

The obtained results were compared with other sorbents used for the same purpose (Table 1). The highest values were reached with wheat bran and banana peel [3,37]. However, it should be pointed out that in this work the adsorption capacities are calculated per gram of sponges and not per gram of oxMWCNTs. This is important since the adsorption of PCs is exclusively due to the oxMWCNTs. Therefore, calculating the  $q_{max}$  considering only the grams of oxMWCNTs a value of 454.55 mg/g is obtained, which is comparable with the most efficient materials. Moreover, the PDMS/oxMWCNTs sponge has the advantages of being user-friendly and easy to manipulate during all the steps of the waste treatment.

**Table 1.** Langmuir constants for PCs adsorption from various absorbents reported in literature.

Adsorbent	$q_{max}$ (mg/g)	$K_L$ (L/g)	References
PDMS/oxMWCNTs	4.39 (454.55)	0.014	This work
Banana peel	688.9	0.24	[3]
Wheat bran	487.3	0.13	[37]
Olive pomace	11.40	0.005	[43]
Activated carbon coated with milk protein	246.45	9.1	[44]
Activated carbon	268.17	0.14	[45]

From the variation of  $K_L$  values with temperature we calculate the Gibbs free energy ( $\Delta G^\circ$ ) of adsorption, enthalpy ( $\Delta H^\circ$ ), and entropy ( $\Delta S^\circ$ ) using the following equation:

$$\Delta G^\circ = -RT \ln(K_{LD}) \quad (6)$$

and the van't Hoff equation:

$$\ln(K_{LD}) = \left( \frac{\Delta S^\circ}{R} \right) - \left( \frac{\Delta H^\circ}{RT} \right) \quad (7)$$

in which  $R$  is the gas constant (8.314 J/(mol K)),  $T$  is the temperature expressed in Kelvin, and  $K_{LD}$  is obtained by multiplying  $K_L$  by 1000 [46,47].

The van't Hoff plot of  $\ln(K_{LD})$  against  $1/T$  evidenced a good linearity with an  $R^2 = 0.96$  and both  $\Delta H^\circ$  and  $\Delta S^\circ$  were calculated (Figure 6). The negative values of  $\Delta G^\circ$  suggests that the process occurs

spontaneously. The positive value of  $\Delta H^\circ$  represents an endothermic reaction while values of  $\Delta S^\circ$  higher than zero evidenced that the randomness increased at the solid liquid interface due to the high affinity of the sorbent for the PCs [46].

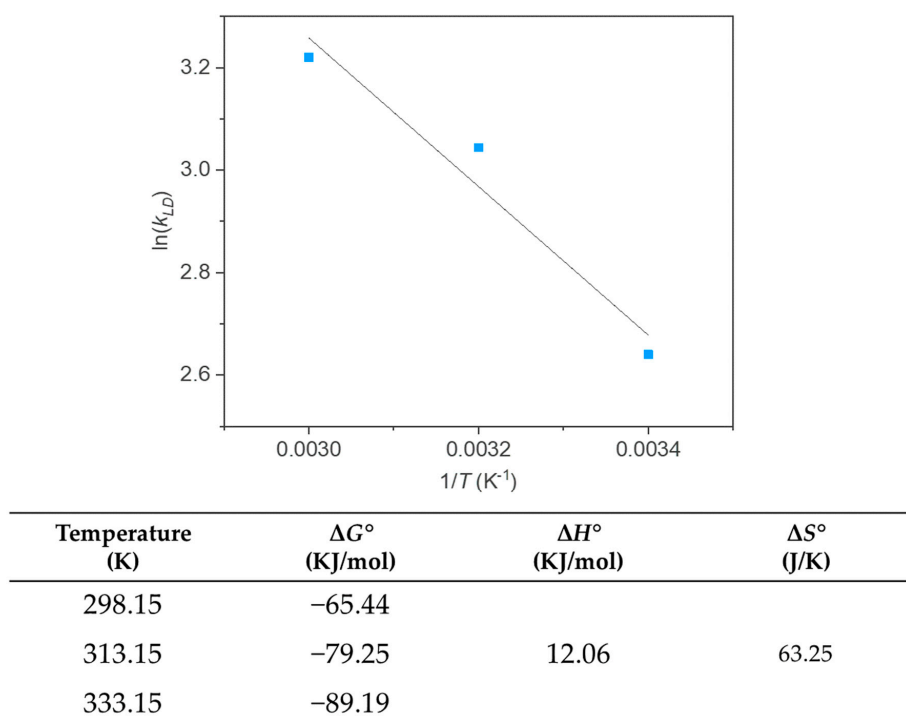


**Figure 6.** Van't Hoff plot for phenols adsorption from OMW. The calculated values from Equation (7) are reported in the table.

### 3.4. Kinetic of the Adsorption Process

To elucidate the adsorption mechanisms in OMW, adsorption kinetics have been evaluated. The mechanism of the adsorption strongly depends on the physical and chemical characteristics of the adsorbent as well as on the mass transport process. Pseudo-first-order and pseudo-second-order equations were examined in this study.

The pseudo-first-order equation [48] is represented by the following equation:

$$\ln(q_e - q_t) = \ln q_e - k_1 t \quad (8)$$

in which  $q_t$  is relative to the number of PCs adsorbed (mg/g) at any time  $t$  (h), and  $k_1$  ( $\text{h}^{-1}$ ) is the equilibrium rate constant of pseudo-first-order sorption. By plotting  $\ln(q_e - q_t)$  against  $t$  a straight line should be obtained with slope  $-K_1$  and intercept  $\ln q_e$ .

The pseudo-second-order equation [49] is expressed in the form:

$$\frac{t}{q_t} = \frac{1}{k_2 q_e^2} + \frac{t}{q_e} \quad (9)$$

in which  $k_2$  is the rate constant of the pseudo-second-order equation ( $\text{g/g h}$ ). The rate constant ( $k_2$ ) and the equilibrium adsorption capacity ( $q_e$ ) can be obtained from the slope and the intercept of the plot of  $t/q_t$  versus  $t$ . The experimental data fitted with both the models are reported in Figure 7.

It is evident that pseudo-second-order kinetic model better describes the experimental data ( $R^2 > 0.99$ ), thus suggesting that chemical sorption, mainly due to  $\pi$ - $\pi$  interactions [28], occurs between the PCs and PDMS/oxMWCNTs sponge [3]



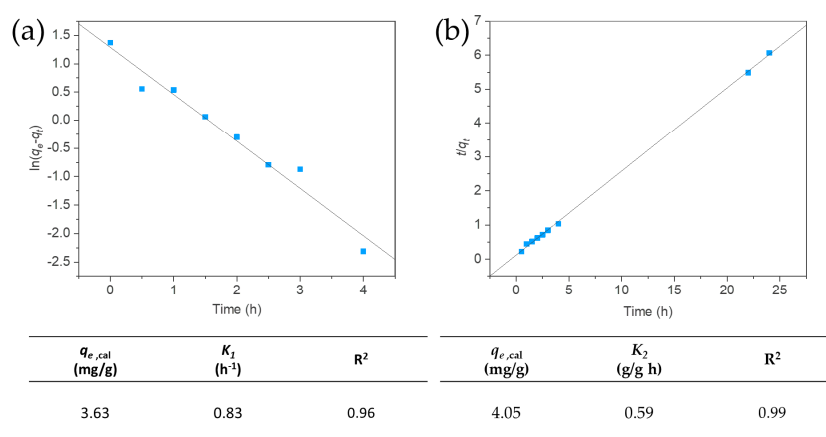


**Figure 7.** Application of (a) pseudo-first-order adsorption model and (b) pseudo-second-order adsorption model. The calculated values from Equations (8) and (9) are reported in the tables under graphs (a) and (b) respectively.

### 3.5. Intraparticle Diffusion Model

The pseudo-first-order and the pseudo-second-order models can explain the adsorption process, but are not useful to identify the diffusion mechanisms.

$$q_t = k_p t^{1/2} + C \quad (10)$$

$k_p$  is the rate constant of intraparticle diffusion model and  $C$  is a constant for any experiment (mg/g). By plotting  $q_t$  versus  $t^{1/2}$  (Figure 8) two linear ranges were observed and ascribed to at least two different diffusion mechanisms of adsorption.

The lower value of  $k_{p2}$  with respect to  $k_{p1}$  (with  $k_{p1}$  and  $k_{p2}$  representing  $k_p$  values for step I and II, respectively) indicated that the free path available for diffusion of PCs inside the sponge became smaller, thus causing the reduction of the diffusion rate [50]. It can be hypothesized that firstly the adsorption occurs on the most accessible sites on the oxMWCNTs surface. Once these sites are saturated, the PCs entered into smaller pores and/or reached the binding sites in the interstitial space between oxMWCNTs, causing a decrease in the diffusion rate [28,32,51].

Interestingly, more than 95% of the total adsorption process occurs at the faster step. Moreover, a higher  $K_p$  value in the first step was obtained with respect to that obtained in aqueous solutions [28], thus confirming that the swelling of the sponge in OMW can speed up the entire adsorption process [30,33].

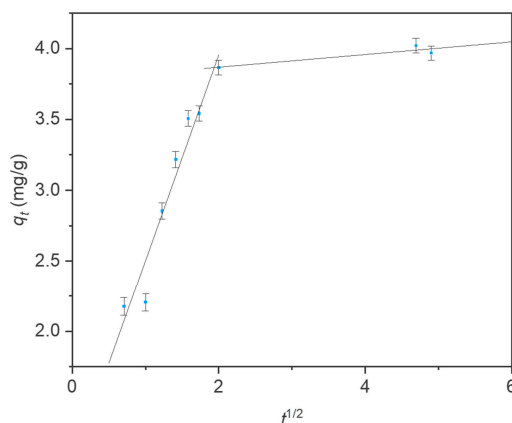


**Figure 8.** Application of intraparticle diffusion model for the adsorption of phenols in OMW onto PDMS/oxMWCNTs sponges.

### 3.6. Desorption and Reusability Studies

Since the chemisorption process occurs between phenols and oxMWCNTs, adsorbed compounds can be removed with an acidic treatment [28]. After the first adsorption process, the PDMS/oxMWCNTs sponges were washed in 10% acetic acid at 60 °C to break the  $\pi$ - $\pi$  interactions. The washing procedure permits the solubilization of most of the adsorbed PCs (~99%) (Figure 9, blue columns), which can thus be used in phenolic-enriched foods after simple further purification steps. Furthermore, the sponge can be reused without losing its adsorption capacity, confirming the high stability of the nanocomposite despite the swelling process. This suggests the possibility to use the nanocomposite for an higher number of adsorption/desorption cycles, thus permitting the decrease of costs for the treatment of OMW with higher phenols concentrations and the complete purification of the waste that can thus be used for fertirrigation [9].

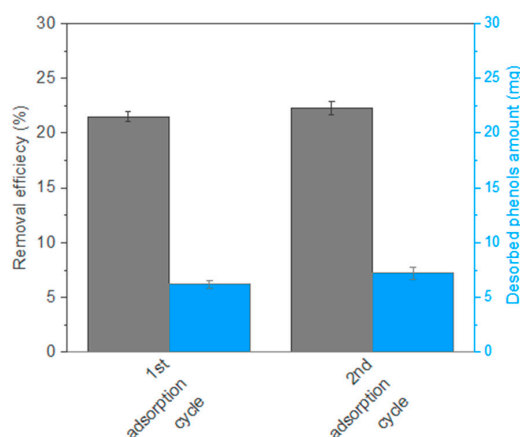


**Figure 9.** Reusability tests for PDMS/oxMWCNTs sponges reporting removal efficiency % (gray column) and the amount of desorbed phenols (blue column).

## 4. Conclusions

The present work describes the application of spongy nanocomposites made of PDMS and oxidized MWCNTs for the adsorption of phenols from olive mill wastewater. The MWCNTs loading was performed with a straightforward method without the use of complex procedures. The oxidation of the nanomaterial was performed directly on the sponge, simplifying the post-treatment and speeding up the whole fabrication process. The entrapped nanomaterials were stable and evidenced good adsorption capacity compared to other systems. The pH of the OMW and pKa of the phenolic compounds can influence the removal efficiency of the nanocomposites. By the evaluation of thermodynamic parameters, we observed that the adsorption process is spontaneous and with a high affinity for the phenolic compounds. The adsorption process in OMW is described by the Langmuir isotherm, suggesting the formation of a monolayer on the nanomaterial surface and evidencing a different behavior of the nanocomposites with respect to what happens in standard aqueous solutions in which the formation of a PCs heterogeneous multilayer on an adsorbent surface was observed. It is also interesting to note that the presence of complex matrices such as OMW can speed up the entire adsorption process (more than 95% of the adsorption is completed in less than 4 h) with respect to standard aqueous solution. We ascribed this behavior to the presence of a small amount of oil inside the OMW that can promote the swelling of the sponge and the diffusion of the mixture inside the polymeric matrices. This is interesting since the oil seasonal production required the fast processing of OMW.

The nanocomposite can thus be easily used to work in batch conditions. This could be useful for a real application of the system. After its production, OMW is stored in a big tank in which the spongy nanocomposites can be added for the adsorption process. Thus, the nanocomposite can be used directly *in situ*. In this view, the entrapment of oxMWCNTs adsorbent in a porous polymeric matrix represents

a significant advantage; in this way, post-treatment processes, such as filtration and/or centrifugation, are not required to remove the adsorbent phase after the adsorption process, decreasing the time and the costs of the treatment. Moreover, the nanomaterial can be easily handled and disposed in a safe way without the use of specialized personnel. The surface of the nanomaterial can be regenerated with a mild treatment with diluted acetic acid. On one hand this permits us to further decrease the costs of production in wastewater treatment. On the other hand, the adsorbed phenolic compound can be easily desorbed from the sponge and can be used, after small further purification, to produce phenolic-enriched food due to its health benefits ranging from reduced incidence of cardiovascular disease, diabetes, and cancers. Furthermore, the treated OMW can be a useful source for fertirrigation. This could permit us to transform a waste product to a resource, especially for the regions of the Mediterranean area in which is concentrated most of the world's production of olive oil. Moreover, the reusability of the material can be useful for OMW with high concentration of phenols that needs repetitive cycles of purification.

**Supplementary Materials:** The following are available online at <http://www.mdpi.com/2073-4441/12/12/3471/s1>, Figure S1: Normalized removal efficiency % data to 0–1 range on the maximal value after 4 h of the uptake process and removal efficiency % at equilibrium for an aqueous solution of phenol and 4-nitrophenol. Figure S2: Fitting of experimental data with linearized Freundlich isotherm model for phenols in OMW ( $R^2 = 0.8$ ).

**Author Contributions:** Conceptualization, A.T.; methodology, A.T. and C.M.; validation, A.T. and C.M.; formal analysis, A.T. and C.M.; investigation, A.T.; resources, A.T. and C.M.; data curation, A.T. and C.M.; writing—original draft preparation, A.T.; writing—review and editing, A.T. and C.M.; supervision, A.T. and C.M.; funding acquisition, A.T. and C.M. All authors have read and agreed to the published version of the manuscript.

**Funding:** This research was funded by Fondazione CARIPUGLIA, project: “Materiali innovativi porosi nanocompositi per la rimozione e il recupero di composti fenolici da acque di vegetazione olearie” and Cohesion fund 2007–2013–APQ Ricerca Regione Puglia “Programma regionale a sostegno della specializzazione intelligente e della sostenibilità sociale ed ambientale-FutureInResearch” under Grant No. 9EC1495 (Ultrasensitive sensor for food analysis).

**Conflicts of Interest:** The authors declare no conflicts of interest. The funders had no role in the design of the study; in the collection, analyses, or interpretation of data; in the writing of the manuscript, or in the decision to publish the results.

## References

1. El-Abbassi, A.; Hafidi, A.; García-Payo, M.C.; Khayet, M. Concentration of olive mill wastewater by membrane distillation for polyphenols recovery. *Desalination* **2009**, *245*, 670–674. [[CrossRef](#)]
2. Della Greca, M.; Monaco, P.; Pinto, G.; Pollio, A.; Previtera, L.; Temussi, F. Phytotoxicity of Low-Molecular-Weight Phenols from Olive Mill Waste Waters. *Bull. Environ. Contam. Toxicol.* **2001**, *67*, 352–359. [[CrossRef](#)] [[PubMed](#)]
3. Achak, M.; Hafidi, A.; Ouazzani, N.; Sayadi, S.; Mandi, L. Low cost biosorbent “banana peel” for the removal of phenolic compounds from olive mill wastewater: Kinetic and equilibrium studies. *J. Hazard. Mater.* **2009**, *166*, 117–125. [[CrossRef](#)] [[PubMed](#)]
4. Sklavos, S.; Gatidou, G.; Stasinakis, A.S.; Haralambopoulos, D. Use of solar distillation for olive mill wastewater drying and recovery of polyphenolic compounds. *J. Environ. Manag.* **2015**, *162*, 46–52. [[CrossRef](#)] [[PubMed](#)]
5. Dutournié, P.; Jeguirim, M.; Khiari, B.; Goddard, M.-L.; Jellali, S. Olive Mill Wastewater: From a Pollutant to Green Fuels, Agricultural Water Source, and Bio-Fertilizer. Part 2: Water Recovery. *Water* **2019**, *11*, 768. [[CrossRef](#)]
6. Schaffer, S.; Podstawa, M.; Visioli, F.; Bogani, P.; Müller, W.E.; Eckert, G.P. Hydroxytyrosol-Rich Olive Mill Wastewater Extract Protects Brain Cells in Vitro and ex Vivo. *J. Agric. Food Chem.* **2007**, *55*, 5043–5049. [[CrossRef](#)]
7. Visioli, F.; Galli, C. The Effect of Minor Constituents of Olive Oil on Cardiovascular Disease: New Findings. *Nutr. Rev.* **2009**, *56*, 142–147. [[CrossRef](#)]
8. Bulotta, S.; Celano, M.; Lepore, S.M.; Montalcini, T.; Pujia, A.; Russo, D. Beneficial effects of the olive oil phenolic components oleuropein and hydroxytyrosol: Focus on protection against cardiovascular and metabolic diseases. *J. Transl. Med.* **2014**, *12*, 219. [[CrossRef](#)]

9. Colarieti, M.L.; Toscano, G.; Greco, G. Toxicity attenuation of olive mill wastewater in soil slurries. *Environ. Chem. Lett.* **2006**, *4*, 115–118. [[CrossRef](#)]
10. Abdelwahab, O.; Nassef, E.M. Treatment of Petrochemical Wastewater Containing Phenolic Compounds by Electrocoagulation Using a Fixed Bed Electrochemical Reactor. *Int. J. Electrochem. Sci.* **2013**, *8*, 1534–1550.
11. Jerman Klen, T.; Mozetič Vodopivec, B. Ultrasonic Extraction of Phenols from Olive Mill Wastewater: Comparison with Conventional Methods. *J. Agric. Food Chem.* **2011**, *59*, 12725–12731. [[CrossRef](#)] [[PubMed](#)]
12. Pelendridou, K.; Michailides, M.K.; Zagklis, D.P.; Tekerlekopoulou, A.G.; Paraskeva, C.A.; Vayenas, D.V. Treatment of olive mill wastewater using a coagulation–flocculation process either as a single step or as post-treatment after aerobic biological treatment. *J. Chem. Technol. Biotechnol.* **2014**, *89*, 1866–1874. [[CrossRef](#)]
13. Hosseini, S.A.; Davodian, M.; Abbasian, A.R. Remediation of phenol and phenolic derivatives by catalytic wet peroxide oxidation over Co-Ni layered double nano hydroxides. *J. Taiwan Inst. Chem. Eng.* **2017**, *75*, 97–104. [[CrossRef](#)]
14. Domingues, E.; Assunção, N.; Gomes, J.; Lopes, D.V.; Frade, J.R.; Quina, M.J.; Quinta-Ferreira, R.M.; Martins, R.C. Catalytic Efficiency of Red Mud for the Degradation of Olive Mill Wastewater through Heterogeneous Fenton's Process. *Water* **2019**, *11*, 1183. [[CrossRef](#)]
15. Amor, C.; Marchão, L.; Lucas, M.S.; Peres, J.A. Application of advanced oxidation processes for the treatment of recalcitrant agro-industrial wastewater: A review. *Water* **2019**, *11*, 205. [[CrossRef](#)]
16. Garcia-Segura, S.; Bellotindos, L.M.; Huang, Y.-H.; Brillas, E.; Lu, M.-C. Fluidized-bed Fenton process as alternative wastewater treatment technology—A review. *J. Taiwan Inst. Chem. Eng.* **2016**, *67*, 211–225. [[CrossRef](#)]
17. Ran, N.; Gilron, J.; Sharon-Gojman, R.; Herzberg, M. Powdered Activated Carbon Exacerbates Fouling in MBR Treating Olive Mill Wastewater. *Water* **2019**, *11*, 2498. [[CrossRef](#)]
18. Kapellakis, I.; Tzanakakis, V.A.; Angelakis, A.N. Land Application-Based Olive Mill Wastewater Management. *Water* **2015**, *7*, 362–376. [[CrossRef](#)]
19. Paraskeva, P.; Diamadopoulos, E. Technologies for olive mill wastewater (OMW) treatment: A review. *J. Chem. Technol. Biotechnol.* **2006**, *81*, 1475–1485. [[CrossRef](#)]
20. Bernal, V.; Giraldo, L.; Moreno-Piraján, J.C. Insight into adsorbate–adsorbent interactions between aromatic pharmaceutical compounds and activated carbon: Equilibrium isotherms and thermodynamic analysis. *Adsorption* **2020**, *26*, 153–163. [[CrossRef](#)]
21. Takahashi, K.; Yoshida, S.; Urkasame, K.; Iwamura, S.; Ogino, I.; Mukai, S.R. Carbon gel monoliths with introduced straight microchannels for phenol adsorption. *Adsorption* **2019**, *25*, 1241–1249. [[CrossRef](#)]
22. Duy Nguyen, H.; Nguyen Tran, H.; Chao, H.-P.; Lin, C.-C. Activated Carbons Derived from Teak Sawdust-Hydrochars for Efficient Removal of Methylene Blue, Copper, and Cadmium from Aqueous Solution. *Water* **2019**, *11*, 2581. [[CrossRef](#)]
23. Nikić, J.; Tubić, A.; Watson, M.; Maletić, S.; Šolić, M.; Majkić, T.; Agbaba, J. Arsenic Removal from Water by Green Synthesized Magnetic Nanoparticles. *Water* **2019**, *11*, 2520. [[CrossRef](#)]
24. Nabeela Nasreen, S.A.A.; Sundarajan, S.; Syed Nizar, S.A.; Ramakrishna, S. Nanomaterials: Solutions to water-concomitant challenges. *Membranes* **2019**, *9*, 40. [[CrossRef](#)] [[PubMed](#)]
25. Nasreen, S.A.A.N.; Sundarajan, S.; Nizar, S.A.S.; Balamurugan, R.; Ramakrishna, S. Advancement in electrospun nanofibrous membranes modification and their application in water treatment. *Membranes* **2013**, *3*, 266–284. [[CrossRef](#)] [[PubMed](#)]
26. Aly, A.A.; Hasan, Y.N.Y.; Al-Farraj, A.S. Olive mill wastewater treatment using a simple zeolite-based low-cost method. *J. Environ. Manag.* **2014**, *145*, 341–348. [[CrossRef](#)] [[PubMed](#)]
27. Frascari, D.; Bacca, A.E.M.; Zama, F.; Bertin, L.; Fava, F.; Pinelli, D. Olive mill wastewater valorisation through phenolic compounds adsorption in a continuous flow column. *Chem. Eng. J.* **2016**, *283*, 293–303. [[CrossRef](#)]
28. Turco, A.; Monteduro, A.; Mazzotta, E.; Maruccio, G.; Malitesta, C. An Innovative Porous Nanocomposite Material for the Removal of Phenolic Compounds from Aqueous Solutions. *Nanomaterials* **2018**, *8*, 334. [[CrossRef](#)]
29. Singleton, V.L.; Orthofer, R.; Lamuela-Raventós, R.M. Analysis of total phenols and other oxidation substrates and antioxidants by means of folin-ciocalteu reagent. *Methods Enzymol.* **1999**, *299*, 152–178. [[CrossRef](#)]
30. Turco, A.; Malitesta, C.; Barillaro, G.; Greco, A.; Maffezzoli, A.; Mazzotta, E. A magnetic and highly reusable macroporous superhydrophobic/superoleophilic PDMS/MWNT nanocomposite for oil sorption from water. *J. Mater. Chem. A* **2015**, *3*, 17685–17696. [[CrossRef](#)]
31. Delor-Jestin, F.; Tomer, N.S.; Singh, R.P.; Lacoste, J. Durability of crosslinked polydimethylsiloxanes: The case of composite insulators. *Sci. Technol. Adv. Mater.* **2008**. [[CrossRef](#)] [[PubMed](#)]

32. Agnihotri, S.; Mota, J.P.B.; Rostam-Abadi, M.; Rood, M.J. Theoretical and experimental investigation of morphology and temperature effects on adsorption of organic vapors in single-walled carbon nanotubes. *J. Phys. Chem. B* **2006**, *110*, 7640–7647. [\[CrossRef\]](#) [\[PubMed\]](#)
33. Turco, A.; Primiceri, E.; Frigione, M.; Maruccio, G.; Malitesta, C. An innovative, fast and facile soft-template approach for the fabrication of porous PDMS for oil–water separation. *J. Mater. Chem. A* **2017**, *5*, 23785–23793. [\[CrossRef\]](#)
34. Turco, A.; Pennetta, A.; Caroli, A.; Mazzotta, E.; Monteduro, A.G.; Primiceri, E.; de Benedetto, G.; Malitesta, C. Easy fabrication of mussel inspired coated foam and its optimization for the facile removal of copper from aqueous solutions. *J. Colloid Interface Sci.* **2019**, *552*, 401–411. [\[CrossRef\]](#) [\[PubMed\]](#)
35. Lin, D.; Xing, B. Adsorption of phenolic compounds by carbon nanotubes: Role of aromaticity and substitution of hydroxyl groups. *Environ. Sci. Technol.* **2008**, *42*, 7254–7259. [\[CrossRef\]](#)
36. Daâssi, D.; Lozano-Sánchez, J.; Borrás-Linares, I.; Belbahri, L.; Woodward, S.; Zouari-Mechichi, H.; Mechichi, T.; Nasri, M.; Segura-Carretero, A. Olive oil mill wastewaters: Phenolic content characterization during degradation by *Coriopsis gallica*. *Chemosphere* **2014**, *113*, 62–70. [\[CrossRef\]](#) [\[PubMed\]](#)
37. Achak, M.; Hafidi, A.; Mandi, L.; Ouazzani, N. Removal of phenolic compounds from olive mill wastewater by adsorption onto wheat bran. *Desalin. Water Treat.* **2014**, *52*, 2875–2885. [\[CrossRef\]](#)
38. Lin, K.; Pan, J.; Chen, Y.; Cheng, R.; Xu, X. Study the adsorption of phenol from aqueous solution on hydroxyapatite nanopowders. *J. Hazard. Mater.* **2009**, *161*, 231–240. [\[CrossRef\]](#)
39. Han, R.; Zou, W.; Li, H.; Li, Y.; Shi, J. Copper (II) and lead (II) removal from aqueous solution in fixed-bed columns by manganese oxide coated zeolite. *J. Hazard. Mater.* **2006**, *137*, 934–942. [\[CrossRef\]](#)
40. Ho, Y.S.; Chiang, C.C. Sorption studies of acid dye by mixed sorbents. *Adsorption* **2001**, *7*, 139–147. [\[CrossRef\]](#)
41. Freundlich, H.M. Over the adsorption in solution. *J. Physicochem.* **1906**, *57*, 385.
42. Langmuir, I. The constitution and fundamental properties of solids and liquids. Part I. Solids. *J. Am. Chem. Soc.* **1916**, *38*, 2221–2295. [\[CrossRef\]](#)
43. Stasinakis, A.S.; Elia, I.; Petalas, A.V.; Halvadakis, C.P. Removal of total phenols from olive-mill wastewater using an agricultural by-product, olive pomace. *J. Hazard. Mater.* **2008**, *160*, 408–413. [\[CrossRef\]](#) [\[PubMed\]](#)
44. Yangui, A.; Abderrabba, M. Towards a high yield recovery of polyphenols from olive mill wastewater on activated carbon coated with milk proteins: Experimental design and antioxidant activity. *Food Chem.* **2018**, *262*, 102–109. [\[CrossRef\]](#)
45. Senol, A.; Hasdemir, İ.M.; Hasdemir, B.; Kurdaş, İ. Adsorptive removal of biophenols from olive mill wastewaters (OMW) by activated carbon: Mass transfer, equilibrium and kinetic studies. *Asia-Pacific J. Chem. Eng.* **2017**, *12*, 128–146. [\[CrossRef\]](#)
46. Ghosal, P.S.; Gupta, A.K. Determination of thermodynamic parameters from Langmuir isotherm constant-revisited. *J. Mol. Liq.* **2017**, *225*, 137–146. [\[CrossRef\]](#)
47. Milonjić, S.K. A consideration of the correct calculation of thermodynamic parameters of adsorption. *J. Serb. Chem. Soc.* **2007**, *72*, 1363–1367. [\[CrossRef\]](#)
48. Lagergren, S. Zur theorie der sogenannten adsorption gelöster stoffe, Kungliga Svenska Vetenskapsakademiens. *Handlingar* **1898**, *24*, 1–39.
49. Blanchard, G.; Maunaye, M.; Martin, G. Removal of heavy metals from waters by means of natural zeolites. *Water Res.* **1984**, *18*, 1501–1507. [\[CrossRef\]](#)
50. Cheng, C.S.; Deng, J.; Lei, B.; He, A.; Zhang, X.; Ma, L.; Li, S.; Zhao, C. Toward 3D graphene oxide gels-based adsorbents for high-efficient water treatment via the promotion of biopolymers. *J. Hazard. Mater.* **2013**, *263*, 467–478. [\[CrossRef\]](#)
51. Pham, X.-H.; Li, C.A.; Han, K.N.; Huynh-Nguyen, B.-C.; Le, T.-H.; Ko, E.; Kim, J.H.; Seong, G.H. Electrochemical detection of nitrite using urchin-like palladium nanostructures on carbon nanotube thin film electrodes. *Sens. Actuators B Chem.* **2014**, *193*, 815–822. [\[CrossRef\]](#)

**Publisher’s Note:** MDPI stays neutral with regard to jurisdictional claims in published maps and institutional affiliations.



© 2020 by the authors. Licensee MDPI, Basel, Switzerland. This article is an open access article distributed under the terms and conditions of the Creative Commons Attribution (CC BY) license (<http://creativecommons.org/licenses/by/4.0/>).